Available online at www.sciencedirect.com
SCIENCE DIRECT
Computer Communications 27 (2004) 1799–1811
computer communications
www.elsevier.com/locate/comcom

Framework based on stochastic L-Systems for modeling IP traffic with multifractal behavior

Paulo Salvador*, António Nogueira, Rui Valadas

Institute of Telecommunications Aveiro, University of Aveiro, Campus de Santiago, 3810-193 Aveino, Portugal

Received 25 June 2004; accepted 25 June 2004
Available online 12 August 2004

Abstract

This paper presents and compares a set of traffic models, and associated parameter fitting procedures, based on so-called stochastic L-Systems, which were introduced by biologist A. Lindenmayer as a method to model plant growth. Starting from an initial symbol, an L-System generates iteratively sequences of symbols, belonging to an alphabet, through successive application of production rules. In a traffic modeling context, the symbols are interpreted as packet arrival rates or mean packet sizes, and each iteration is associated to a finest time scale of the traffic. These models are able to capture the multiscaling and multifractal behavior sometimes observed in Internet traffic. We describe and compare four traffic models, one characterizing the packet arrival process, and the other three characterizing both the packet arrival and the packet size processes. The models are tested with several measured traffic traces: the well-known pOct Bellcore, a trace of aggregate WAN traffic and two traces of specific applications (Kazaa and Operation Flashing Point). We assess the multifractality of these traces using Linear Multiscale Diagrams. The traffic models are evaluated by comparing, for the measured traffic and for traffic generated according to the inferred models, the probability mass function, the autocovariance function and the queuing behavior. Our results show that the L-System based traffic models that characterize both the packet arrival and packet size processes can achieve very good fitting performance in terms of first- and second-order statistics and queuing behavior.

Keywords: Traffic modeling; Multifractal; Multiscaling; Internet traffic; L-System

1. Introduction

Traffic modeling has an increasing importance in the management and dimensioning of telecommunications networks. Traffic models are used, for example, in the dimensioning of links and buffers (while taking into account statistical multiplexing effects) and in performance analysis of networks. In the Internet, the complexity associated to the mechanisms for traffic generation and control, as well as the diversity of applications and services, have introduced several peculiar behaviors in the traffic, such as self-similarity, long-range dependence and multifractality. These behaviors have a significant impact on the network performance and, therefore, need to be adequately characterized.

Accurate modeling of Internet traffic also requires the characterization of both the packet arrival and the packet size processes [1]. In particular, this is important for accurate prediction of the queuing behavior (i.e. the packet loss ratio or average packet delay suffered on a network node). The queuing behavior addresses the effect of traffic on network performance, and is one of the most important criteria to assess the suitability of traffic models (and associated parameter fitting procedures). Here, the analysis consists in comparing the curves of packet loss ratio (or average packet delay) versus buffer size, obtained with the measured traces (through trace-driven simulation) and with the inferred traffic model (using again trace-driven simulation or numerical computation of the performance measures whenever possible). When dealing with models that characterize only the arrival process, it is common practice to assume that the packet size is fixed and equal to the average packet size of the measured trace. This may lead to large errors when the packets have variable size, such as in IP traffic.

* Corresponding author.
E-mail addresses: salvador@av.it.pt (P. Salvador), nogueira@av.it.pt (A. Nogueira), rv@det.ua.pt (R. Valadas).

0140-3664/$ - see front matter © 2004 Elsevier B.V. All rights reserved.
doi:10.1016/j.comcom.2004.06.014

Recent analysis of measured Internet WAN traffic has revealed that multifractal structures, such as random cascades, can help explaining the scaling behavior typically associated to networking mechanisms operating on small time scales (e.g. TCP flow control). A cascade (or multiplicative process) is a process that fragments a set into smaller and smaller components according to a fixed rule, and at the same time fragments the measure of the components by another (possibly random) rule. Random cascades were introduced by Mandelbrot as a physical model for turbulence [2]. In the traffic modeling context, the set can be interpreted as a time interval and the measure as the number of arrivals or number of bytes (in that interval).

The multifractal nature of network traffic was first noticed by Riedi and Lévy Véhel [3]. Subsequently, various studies have addressed the characterization and modeling of multifractal traffic, essentially within the framework of random cascades [4–11]. Feldmann et al. [4,9] proposed conservative cascades, which are closely related with random cascades, as a model for Internet WAN traffic. They provided plausible physical explanations supporting the adoption of conservative cascades and developed tools to analyze the scaling behavior of this type of cascades. Gao and Rubin considered two extensions of the conservative cascade model: they introduced a dual cascade model, where one cascade characterizes packet inter-arrivals and the other packet sizes [8]; moreover, they considered a cascade model for the counting process representing the aggregation of the packet arrival and packet size processes, i.e. the number of bytes arriving in every time interval [12]. The latter model precludes estimating the packet loss ratio, since the detail of packet sizes is lost through aggregation.

In this paper, we propose a set of traffic models, and associated fitting procedures, capable of capturing multifractal behavior. The traffic models are based on stochastic Lindenmayer-Systems (hereafter referred to as L-Systems). L-Systems are string rewriting techniques which were introduced by biologist A. Lindenmayer in 1968 as a method to model plant growth [13]. They are characterized by an alphabet, an axiom and a set of production rules, and can be used to generate fractals [14]. The alphabet is a set of symbols; the production rules define transformations of symbols into strings of symbols; starting from an initial string (the axiom), an L-System constructs iteratively sequences of symbols through replacement of each symbol by the corresponding string according to the production rules. If the production rules are random, the L-System is called a stochastic L-System. When compared with conservative cascades, stochastic L-Systems introduce a dependence on the construction process (due to the production rules), that has a meaningful physical explanation, and can help understanding the joint impact of network mechanisms and resource limitations on observed traffic [15].

The application of stochastic L-Systems in the traffic modeling context was first introduced by the authors in Ref. [15]. The model proposed in this first work only addressed the characterization of the packet arrival process. In this paper, it will be called the single L-System model. This model is relevant for traffic with fixed packet size, such as ATM traffic and IP, traffic of specific applications where the packet sizes remain approximately constant (e.g. V61P). Three subsequent extensions addressed the characterization of both the packet arrival and packet size processes. The first extension introduced a model with two independent L-Systems, one for the packet arrival and the other for the packet size processes, called double L-System model [16]. Due to the independence of the two L-Systems, this model is not able to capture the correlations between arrivals and sizes, although it captures multifractal behavior on both packet arrivals and packet sizes. The second extension was based on a single bi-dimensional L-System, where the alphabet elements are pairs of arrival rates and mean packet sizes, called the joint L-System model [17]. Opposite to the previous model, this one is able to capture correlations between arrivals and sizes. One disadvantage, however, is that it may require a large number of parameters. Also, the multifractal behavior is only captured in the (aggregate) byte arrival process. This paper introduces a third extension, which was devised in order to allow a lower number of parameters and also to provide a more detailed modeling of the packet size. In this case, only the packet arrival process is modeled through an L-System. The characterization of the packet size is performed by associating, at the finest time scale, a probability mass function (PMF) (of packet sizes) to each packet arrival rate [18]. In this way the model is able to capture correlations between packet arrivals and packet sizes, and multifractal behavior on packet arrivals (but not on packet sizes). Note that in this extension the packet sizes are characterized individually, whereas in the previous ones, only the mean packet sizes were modeled. This model will be called the L-System with PMFs.

This paper is organized as follows. In Section 2 we give the required background on L-Systems. In Sections 3 and 4 we present the traffic models and describe the associated fitting procedures. In Section 5 we discuss the results of applying the different procedures to measured traffic traces. Finally, Section 6 presents the conclusions.

2. L-Systems background

The basic idea behind L-Systems is to define complex objects by successively replacing parts of a simple object using a set rules. The L-System is a feedback machine that operates on strings of symbols. The set of symbols is called the alphabet. Starting from an initial state (called axiom), an L-System operates, at each iteration, by applying the set of production (or rewriting) rules simultaneously to all symbols of an input string to give an output string. For a comprehensive introduction to L-Systems see the book by Peitgen et al. [14].

Consider a simple example of an organism growing through cell subdivisions. There are two types of cells represented by letters A and B. Cell subdivisions are modeled by replacing these symbols with strings of symbols: cell A subdivides into two cells represented by string AB; cell B subdivides into two cells represented by string AA. The ordering of the symbols is relevant in an L-System. The organism modeled by this L-System grows by repeated cell subdivisions. At birth the organism is the single cell A. After one subdivision the organism has two cells represented by string AB. After two subdivisions, the organism has four cells given by string ABAA, and after three subdivisions the organism has eight cells represented by string ABAAABAB. Using the formalism of L-Systems this growth process can be described as:

Alphabet: {A,B}
Axiom: A
Rules: $A \rightarrow AB$
$B \rightarrow AA$

The production rules can be stochastic. In stochastic L-Systems, there may be several production rules for one symbol, and the specific rule is selected according to a probability distribution. Taking previous example, one production rule could be to convert A into AB with probability 0.4 or into BB with probability 0.6 (instead of converting always A into AB). In this case, after three iterations several strings are possible, e.g. ABAAABAB, ABABBBAB, or AAAAABBB. Stochastic L-Systems are a method to construct recursively random sequences with multifractal behavior [14].

As another example, consider the following stochastic L-System:

Alphabet: $\{X_1,X_2,X_3,X_4,X_5\}$
Axiom: X_3
Rule 1: $X_1 \rightarrow X_1X_1$
Rule 2: $X_2 \rightarrow X_1X_3$, with prob. 1/3
$X_2 \rightarrow X_3X_1$, with prob. 1/3
$X_2 \rightarrow X_2X_2$, with prob. 1/3
Rule 3: $X_3 \rightarrow X_3X_3$, with prob. 1/5
$X_3 \rightarrow X_2X_4$, with prob. 1/5
$X_3 \rightarrow X_4X_2$, with prob. 1/5
$X_3 \rightarrow X_1X_5$, with prob. 1/5
$X_3 \rightarrow X_5X_1$, with prob. 1/5
Rule 4: $X_4 \rightarrow X_3X_5$, with prob. 1/3
$X_4 \rightarrow X_5X_3$, with prob. 1/3
$X_4 \rightarrow X_4X_4$, with prob. 1/3
Rule 5: $X_5 \rightarrow X_5X_5$

The alphabet elements of this L-System can be associated to graphical elements. For example, X_i can represent a rectangle with an area of i units. The L-System production rules assure that the average area of the child rectangles is equal to the area of its parent rectangle. Some of the possible outcomes of the L-System construction are represented in Fig. 1.

In order to build a network traffic model, the area of a rectangle can be interpreted as the amount of traffic (number of arrivals or number of bytes), observed in a particular time interval. This is precisely the idea behind the proposed traffic model, that will be described in Section 3.

3. Traffic models

3.1. Single L-System

We first describe the traffic model based on a single L-System, that characterizes the packet arrival process. The single L-System is defined by an alphabet of arrival rates

$$\Lambda = \{\lambda_1, \lambda_2, \ldots, \lambda_L\}, \quad \lambda_i \in \mathbb{R}_0^+, \quad i = 1, \ldots, L, \tag{1}$$

by production rules that randomly generate two arrival rates from a previous one and by an axiom which is a predefined initial arrival rate. Without loss of generality, we assume $\lambda_1 < \lambda_2 < \cdots < \lambda_L$.

The packet arrival process is constructed progressively, governed by an L-System machine, where each iteration produces a new time scale. Starting with the coarsest time

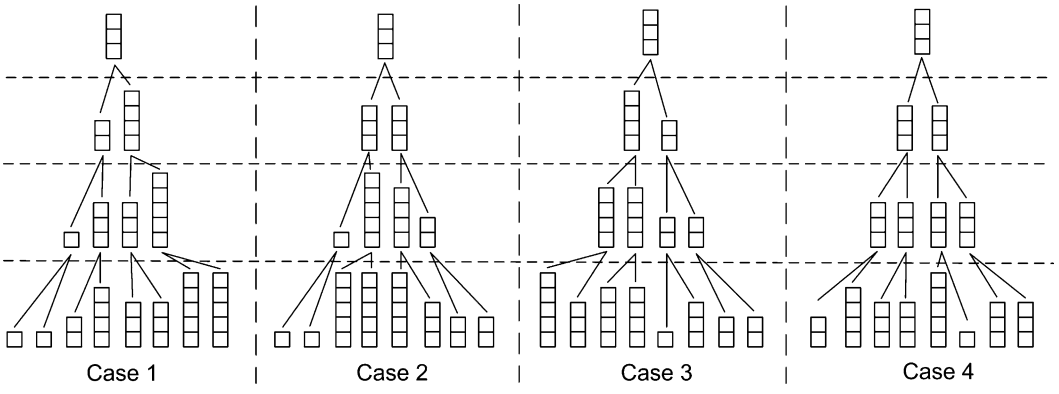

Fig. 1. Example of stochastic L-System with rectangles.

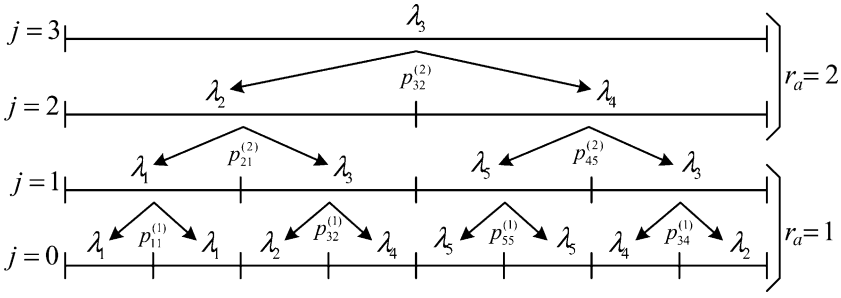

Fig. 2. Construction of the traffic process based on the single L-System.

scale, where traffic is characterized by a single arrival rate over a single time interval, each iteration generates a finest time scale by (i) division of each (parent) time interval in two new equal length (child) subintervals and (ii) association of arrival rates to each new subinterval according to the production rules of the stochastic L-System. We allow the grouping of time scales in time scale ranges and the definition of different sets of production rules for each time scale range. This is motivated by the fact that each set of production rules maps into a distinct scaling behavior [19]. Classically, there will be scaling if the log–log plot of the qth order energies (usual energy is $q=2$) as a function of scale behaves linearly; if the plot is (globally) non-linear, different time scale ranges can be detected where linearity is observed (see, for example, Ref. [7]). The packet arrival process construction is shown in Fig. 2.

To characterize the packet arrival process we define $X^{(i)}_{(j,r_a)} \in \Lambda$ as the arrival rate at time interval i of time scale j and time scale range r_a. Let the number of scales be S and the number of ranges of scales be R_a. For convenience, we let j decrease from $j=S-1$ (at the coarsest time scale) to $j=0$ (at the finest time scale).

Also, we let r_a decrease from $r_a=R_a$ (the range of coarsest time scales) to $r_a=1$ (the range of finest time scales). Thus, the number of time intervals at time scale j, which we will denote by N_j, is 2^{S-j-1}. Moreover, assuming a unitary width for the intervals of the finest time scale, $j=0$, the width at scale j will be 2^j. To relate time scales and time scale ranges we define j_{r_a} as the coarsest scale j in range r_a. Thus, in Fig. 2, $S=4$, $R_a=2$, $j_2=3$ and $j_1=1$.

In order to assure that the average arrival rate is the same in all time scales, so as to maintain physical meaning, we will impose the following condition to the production rules:

$$X^{(i)}_{(j,r_a)} = \tfrac{1}{2} X^{(2i-1)}_{(j-1,r'_a)} + \tfrac{1}{2} X^{(2i)}_{(j-1,r'_a)}, \tag{2}$$

i.e. the mapping of arrival rates is such that the arrival rate averaged over the left and right child subintervals will be equal to the parent arrival rate. This will be called the mass preservation property. With this condition, the traffic process generation can be described by axiom $X^{(1)}_{(S-1,R_a)}$, the arrival rate at the coarsest time scale, and production rules defined by

$$X^{(i)}_{(j,r_a)} = \lambda_l \overset{p^{(r_a)}_{lq}}{\rightarrow} \begin{cases} X^{(2i-1)}_{(j-1,r'_a)} = \lambda_q, \\ X^{(2i)}_{(j-1,r'_a)} = 2\lambda_l - \lambda_q, \end{cases} \tag{3}$$

where $\sum_{q=1}^{L} p^{(r_a)}_{lq} = 1, \forall l$. Thus, an arrival rate λ_l in interval i, scale j and range r_a produces, with probability $p^{(r_a)}_{lq}$, arrival rate λ_q at the left subinterval $2i-1$ and arrival rate $2\lambda_l-\lambda_q$ at the right subinterval $2i$, of next scale $j-1$ and range r'_a. The production rules can be totally described by R_a $L\times L$ matrices

$$\mathbf{P}^{(r_a)} = (p^{(r_a)}_{lq}), \quad l,q = 1,\ldots,L, \quad r_a = 1,\ldots,R_a. \tag{4}$$

In order to guarantee that the alphabet is closed with respect to the production rules, we impose the following conditions: (i) $\lambda_i - \lambda_{i-1} = (\lambda_L - \lambda_1)/(L-1)$, $i=2,3,\ldots,L$, i.e the λ_i values will be equidistant; (ii) $p^{(r_a)}_{lq} = 0$, if $q > l + \min(L-l, l-1)$ or $q < l - \min(L-l, l-1)$.

Finally, the L-System construction defines, at scale j and range r_a, the time series

$$Z_{(j,r_a)} = \{X^{(i)}_{(j,r_a)}, i = 1,\ldots,N_j\}. \tag{5}$$

3.2. Double L-System

To characterize both the packet arrival and packet size processes, we first consider a traffic model based on two independent L-Systems, where one L-System describes packet arrivals and the other mean packet sizes. The L-System describing the packet arrival process is equal to the one presented in Section 3.1. The L-System describing the packet size process is defined by an alphabet of mean packet sizes

$$\Gamma = \{\gamma_1, \gamma_2, \ldots, \gamma_G\}, \quad \gamma_i \in \mathbb{R}^+_0, \quad i = 1,\ldots,G, \tag{6}$$

by production rules that randomly generate two mean packet sizes from a previous one and by an axiom which is a predefined initial mean size. Without loss of generality, we assume $\gamma_1 < \gamma_2 < \cdots < \gamma_G$.

The traffic process construction follows the same steps of the single L-System one, except that now each time interval is associated to both a packet arrival rate and a mean packet size, generated by each of the independent L-Systems. We allow the ranges of time scales of mean sizes to be different

from those of arrival rates. The time scale ranges for mean sizes will be denoted by r_s and the number of time scale ranges by R_s. To relate time scales and time scale ranges for mean sizes, we define j_{r_s} as the coarsest scale j in range r_s. To characterize the traffic process we define the pair $(X^{(i)}_{(j,r_a)}, Y^{(i)}_{(j,r_s)})$, where $X^{(i)}_{(j,r_a)} \in \Lambda$ and $Y^{(i)}_{(j,r_s)} \in \Gamma$ are the packet arrival rate and the mean packet size at time interval i of time scale j and time scale ranges r_a for arrivals and r_s for sizes, respectively.

Note that there can be a different scaling phenomena for the arrival and packet size processes, driven by the diverse mechanisms that are involved in the traffic generation and control at the various time scales. Consider, for example, the traffic generated at the user level by an HTTP access. The arrival process depends mainly on the frequency of clicks. However, the packet sizes and flow durations depend mainly on the type of clicks and are independent of the frequency of clicks. For example, the download of a large file generates many large packets and the download of a WWW page generates a few small packets. This motivates allowing different time scale ranges for the packet arrival and packet size processes.

The mass conservation property also holds in the case of mean packet sizes. Thus,

$$Y^{(i)}_{(j,r_s)} = \frac{1}{2}\, Y^{(2i-1)}_{(j-1,r'_s)} + \frac{1}{2} Y^{(2i)}_{(j-1,r'_s)}, \tag{7}$$

i.e. the mapping of mean sizes is such that the mean size averaged over the left and right child subintervals will be equal to the parent mean size.

The generation of mean sizes can be described by axiom $Y^{(1)}_{(s-1,R_s)}$, the mean size at the coarsest time scale, and by production rules defined by

$$Y^{(i)}_{(j,r_s)} = \gamma_m \overset{v^{(r_s)}_{mn}}{\rightarrow} \begin{cases} Y^{(2i-1)}_{(j-1,r'_s)} = \gamma_n, \\ Y^{(2i)}_{(j-1,r'_s)} = 2\gamma_m - \gamma_n, \end{cases} \tag{8}$$

where $\sum_{n=1}^{G} v^{(r_s)}_{mn} = 1, \forall m$. Thus, a mean size γ_m in interval i, scale j and range r_s produces, with probability $v^{(r_s)}_{mn}$, mean size γ_n at the left subinterval $2i-1$ and mean size $2\gamma_m - \gamma_n$ at the right subinterval $2i$, of next scale $j-1$ and range r'_s. The production rules of mean packet sizes can be totally described by R_s $G \times G$ matrices

$$\mathbf{V}^{(r_s)} = (v^{(r_s)}_{mn}), \quad m,n = 1,\ldots,G, \quad r_s = 1,\ldots,R_s. \tag{9}$$

The closure property must also hold in this case. Thus, (i) $\gamma_i - \gamma_{i-1} = (\gamma_G - \gamma_1)/(G-1)$, $i = 2,3,\ldots,G$; (ii) $v^{(r_s)}_{mn} = 0$, if $n > m + \min(G-m, m-1)$ or $n < m - \min(G-m, m-1)$.

Finally, the traffic process at scale j can be defined by time series

$$Z_{(j,r_a,r_s)} = \{(X^{(i)}_{(j,r_a)}, Y^{(i)}_{(j,r_s)}), i = 1,\ldots,N_j\}. \tag{10}$$

Note that it is not possible to have mass conservation simultaneously in the three processes of packet arrivals, byte arrivals and packet sizes using finite alphabets. In our approach, except for a trivial case, the mass conservation property does not hold for the byte arrival process. In fact, the number bytes in a parent interval, which is given by $X^{(i)}_{(j,r_a)} Y^{(i)}_{(j,r_s)} \Delta 2^j$, will not be equal to the sum of bytes in the corresponding child intervals, given by

$$\begin{aligned} &[X^{(2i-1)}_{(j-1,r'_a)} Y^{(2i-1)}_{(j-1,r'_s)} + X^{(2i)}_{(j-1,r'_a)} Y^{(2i)}_{(j-1,r'_s)}] \Delta 2^{j-1} \\ &\quad = [2X^{(i)}_{(j,r_a)} Y^{(i)}_{(j,r_s)} + X^{(2i-1)}_{(j-1,r'_a)} Y^{(2i-1)}_{(j-1,r'_s)} - X^{(i)}_{(j,r_a)} Y^{(2i-1)}_{(j-1,r'_s)} \\ &\qquad - X^{(2i-1)}_{(j-1,r'_a)} Y^{(i)}_{(j,r_s)}] \Delta 2^j, \end{aligned} \tag{11}$$

due to the imposition of mass conservation on arrival rates and mean sizes. Conservation of bytes occurs only in the special case of $X^{(i)}_{(j,r_a)} = X^{(2i-1)}_{(j-1,r'_a)}$ or $Y^{(i)}_{(j,r_a)} = Y^{(2i-1)}_{(j-1,r'_a)}$, i.e. when the arrival rates or the mean sizes of the parent and child. intervals are the same.

3.3. Joint L-System

In this traffic model, a single bi-dimensional L-System is used to characterize jointly the packet arrival and packet size processes. The joint L-System is defined by an alphabet of pairs, where one pair element is a packet arrival rate, λ_l, and the other is a mean packet size, γ_g, i.e.

$$\Omega = \{(\lambda_l, \gamma_g) : \lambda_l \in \Lambda, \gamma_g \in \Gamma\}, \tag{12}$$

by production rules that randomly generate two pairs (of arrival rates and mean sizes) from a previous one and by an axiom which is a predefined initial pair.

The construction of the traffic process follows directly the case of the single L-System. Here, the time scale ranges are defined based on the byte arrival process (process of arrival rates times mean sizes, in bytes/seconds). We denote a time scale range by r_b and the number of time scale ranges by R_b. To relate time scales and time scale ranges, we define j_{r_b} as the coarsest scale j in range r_b. To characterize the traffic process we define the pair $(X^{(i)}_{(j,r_b)}, Y^{(i)}_{(j,r_b)}) \in \Omega$, as the arrival rate and mean size at time interval i of time scale j and time scale range r_b. The traffic process construction is shown in Fig. 3.

As in the case of the previous two models, both the mass conservation and the closure properties hold. The generation of arrival rates and mean sizes can be described by axiom $(X^{(1)}_{(S-1,R_6)}, Y^{(1)}_{(S-1,R_6)})$, the pair of arrival rate and mean size at the coarsest time scale, and by production rules defined by

$$\begin{aligned} &(X^{(i)}_{(j,r_b)}, Y^{(i)}_{(j,r_b)}) \\ &\quad = (\lambda_l, \gamma_m) \overset{u^{(r_b)}_{lmqn}}{\rightarrow} \begin{cases} (X^{(2i-1)}_{(j-1,r'_b)}, Y^{(2i-1)}_{(j-1,r'_b)}) = (\lambda_q, \gamma_n), \\ (X^{(2i)}_{(j-1,r'_b)}, Y^{(2i)}_{(j-1,r'_b)}) = (2\lambda_l - \lambda_q, 2\gamma_m - \gamma_n), \end{cases} \end{aligned} \tag{13}$$

where $\sum_{q=1}^{L} \sum_{n=1}^{G} u^{(r_b)}_{lmqn} = 1, \forall l, \forall m$. Thus, a pair with arrival rate λ_l and mean size γ_m in interval i, scale j and range r_b produces, with probability $u^{(r_b)}_{lmqn}$, a pair with arrival

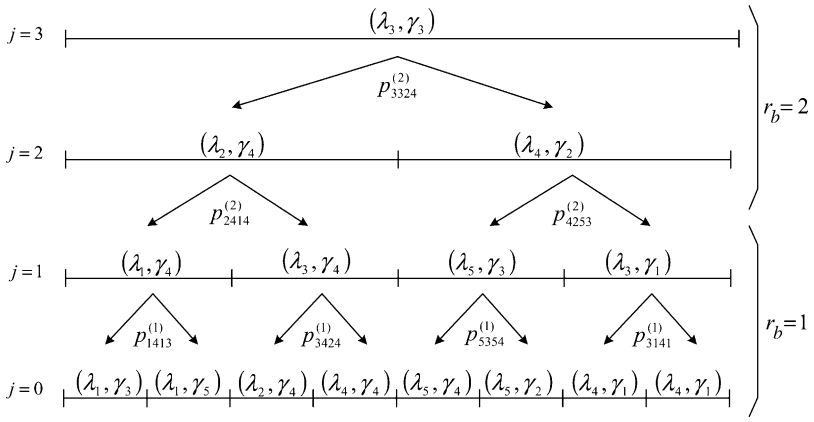

Fig. 3. Construction of the traffic process based on the joint L-System.

rate λ_q and mean size γ_n at the left subinterval $2i-1$ and arrival rate $2\lambda_l-\lambda_q$ and mean size $2\gamma_m-\gamma_n$ at the right subinterval $2i$, of next scale $j-1$ and range r'_b. The production rules can be totally described by the R_b matrices with dimension $L\times G\times L\times G$, $\mathbf{U}^{(r_b)}=(u^{(r_b)}_{lmqn})$, with $l,q=1,\ldots,L$, $m,n=1,\ldots,G$ and $r_b=1,\ldots,R_b$.

Finally, the traffic process at scale j and range r_b can be defined by time series

$$Z_{(j,r_b)}=\{(X^{(i)}_{(j,r_b)},Y^{(i)}_{(j,r_b)}),i=1,\ldots,N_j\}. \tag{14}$$

3.4. L-System with PMFs

This traffic model resorts to a single L-System to characterize the packet arrival process and to a set of discrete distributions to characterize the packet size process. The packet size is characterized only at the finest time scale. Moreover, contrarily to the previous two models, the L-System with PMFs characterizes the individual packet size, instead of the mean packet size computed over a time interval. In this scale, each possible arrival rate is assigned a PMF describing the packet sizes. Thus, there will be a total of L PMFs.

To characterize the packet size process, let E_l be a discrete random variable representing the (individual) packet size associated to arrival rate λ_l. We define L PMFs, one for each packet arrival rate, given by $h^l(e)=P(E_l=e)$, with $e\in\Upsilon^l=\{v_1,v_2,\ldots,v_{Q_l}\}$ and $l=1,2,\ldots,L$; Υ^l is the set of Q_l packet sizes associated with arrival rate λ_l. Note that all packets arriving in a time interval with associated arrival rate λ_l, will be assigned a packet size according to PMF h^l.

The generation of the complete traffic process has three steps: (i) we first generate the sequence of arrival rates at the finest time scale given by the corresponding L-System; (ii) second, within each time interval, the packet arrival instants are spaced uniformly (the number of arrivals is set according to the arrival rate of the interval); (iii) at last, the sizes of all packets are determined, based on PMFs of the[associated arrival rates.

4. Fitting procedures

4.1. Single L-System

The fitting procedure determines the parameters of the single L-System from a data trace. It starts by fixing a sampling interval Δ and considering the time series representing the total number of packet arrivals in each non-overlapping sampling interval. Let this (empirical) time series be $\{A_k,k=1,2,\ldots,K\}$, where A_k represents the number of arrivals in sampling interval k. For convenience, we take the length of the time series K to be a power of 2.

The inference procedure can then be divided into four steps: (i) determination of the L-System alphabet and axiom, (ii) identification of the time scale ranges and (iii) inference of the L-System production rules. The general flow diagram for a L-System fitting procedure is represented in Fig. 4.

There are several possible strategies to infer the L alphabet elements. One choice is to consider the L equidistant arrival rate values, ranging from the minimum to the maximum values of the measured data. However, it is important to include in the alphabet the mean arrival rate of the measured data. Thus, we infer the alphabet with L elements $\{\lambda_i,i=1,2,\ldots,L\}$ such that (i) the L elements are equidistant, i.e. $\lambda_{i+1}-\lambda_i=\delta>0$, $i=1,2,\ldots,L-1$, (ii) the mean arrival rate of data is included in the alphabet, i.e. $\exists i{:}\lambda_i=\text{mean}(A_k/\Delta)$, $i=1,2,\ldots,L$, and (iii) the minimum and the maximum values of data are within the range of the alphabet, i.e. $\lambda_1\le\min(A_k/\Delta)$, $\lambda_L\ge\max(A_k/\Delta)$. The value of L is a compromise between accuracy and complexity.

Due to the mass preservation property, the axiom is inferred as the average arrival rate of $\{A_k\}$, rounded to the closest alphabet element, i.e.

$$X^{(1)}_{(S-1,R_a)}=\Phi_\Lambda\left((1/K\Delta)\sum_{k=1}^{K}A_k\right), \tag{15}$$

where $\Phi_A(x)$ represents a function that rounds x towards the nearest element of A.

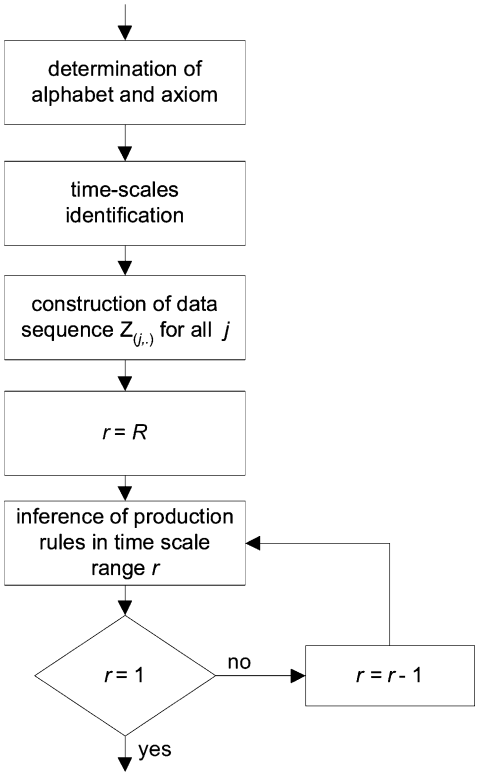

Fig. 4. General flow diagram of a L-System inference procedure.

The identification of time scale ranges is based on wavelet scaling analysis. We use the method proposed by Abry et al. [7], which resorts to the (second-order) logscale diagram. A (second-order) logscale diagram is a plot of energies against scale j, together with confidence intervals about the energies, where these values are a function of the wavelet discrete transform coefficients at scale j. The time scale ranges correspond to the set of time scales for which, within the limits of the confidence intervals, the energies fall on a straight line, i.e. the scaling behavior is linear in a time scale range. Fig. 5 shows the logscale diagram of a trace measured at the University of Aveiro (which is described in Section 5), with 95% confidence intervals. There are three time scale ranges (within a total of 17 time scales) defined by $j_1 = 2, j_2 = 8$ and $j_3 = 17$. Note that, with this method, it is not possible to estimate the energies up to the last specified time scale, due to lack of precision resulting from boundary effects. Specifically, in our case, it was not possible to estimate the energies for $j > 12$, as shown in Fig. 5. However, the usual procedure is to assume that the alignment holds up to the highest specified time scale.

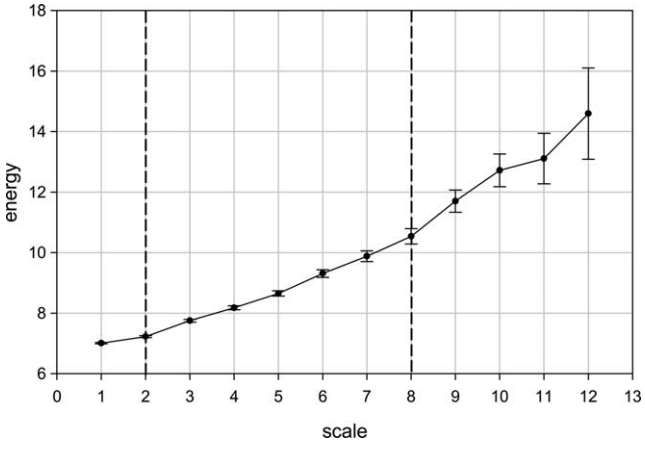

Fig. 5. Second-order logscale diagram, with 95% confidence intervals, trace UA.

The next step is the inference of the L-System production rules, which are fully characterized by the $\mathbf{P}^{(r_a)}$, $r_a = 1, \ldots, R_a$ matrices. First, data is rounded in order to define sequence $Z_{(j,r_a)}$ at each time scale. This comprises obtaining the arrival rates $X^{(i)}_{(j,r_a)}$ from $\{A_k\}$ through

$$X^{(i)}_{(j,r_a)} = \Phi_{\Delta}\left((N_j/K\Delta)\sum_{k=K(i-1)/N_j+1}^{Ki/N_j} A_k\right), \tag{16}$$

with $i = 1,\ldots,N_j$, for each j. Finally, letting $c^{(r_a)}_{lq}$ represent the number of times that, at scale j and range r_a, the parent $X^{(i)}_{(j,r_a)} = \lambda_l$ produced the left child $X^{(2i-1)}_{(j-1,r'_a)} = \lambda_q$, the production rule probabilities can be inferred as

$$p^{(r_a)}_{lq} = c^{(r_a)}_{lq} \Big/ \sum_{q=1}^{L} c^{(r_a)}_{lq}, \quad l = 1,\ldots,L, \quad r_a = 1,\ldots,R_a. \tag{17}$$

4.2. Double L-system

The fitting procedure of the double L-System comprises determining the parameters of the two independent L-Systems characterizing the arrival rates and the mean sizes. We start by constructing the (empirical) time series $\{(A_k,B_k), k = 1,2,\ldots,K\}$, where A_k and B_k represent the number of arrivals and the mean packet size in sampling interval k. After this, the parameters of the two L-Systems are inferred separately through the procedure described in Section 4.1 (and shown in Fig. 4) applied to time series $\{A_k\}$ and $\{B_k\}$, respectively.

In the case of the L-System characterizing the packet size process, the alphabet is inferred as G equidistant mean packet size values such that one alphabet element coincides with the mean packet size of data and the minimum and the maximum values of data are within the range of the alphabet. The axiom is inferred as the mean of $\{B_k\}$, rounded to the closest alphabet element, i.e.

$$Y^{(1)}_{(S-1,R_s)} = \Phi_{\Gamma}\left((1/K)\sum_{k=1}^{K} B_k\right). \tag{18}$$

The identification of time scale ranges is again based on the (second-order) logscale diagram. The production rules, defined by matrices $\mathbf{V}^{(r_s)}$, $r_s = 1,\ldots,R_s$, are inferred by

rounding the empirical times series $\{B_k\}$ to obtain

$$Y_{(j,r_s)}^{(i)} = \Phi_I\left((N_j/K)\sum_{k=K(i-1)N_j+1}^{Ki/N_j} B_k\right), \tag{19}$$

with $i=1,\ldots,N_j$, for each j, and then determining the probabilities through

$$v_{mn}^{(r_s)} = d_{mn}^{(r_s)} \Big/ \sum_{n=1}^{G} d_{mn}^{(r_s)}, \quad m=1,\ldots,G, \quad r_s=1,\ldots,R_s, \tag{20}$$

where $d_{mn}^{(r_s)}$ represents the number of times that, over all scales of range r_s, the parent $Y_{(j,r_s)}^{(i)}=\gamma_m$ produced the left child $Y_{(j-1,r_s')}^{(2i-1)}=\gamma_n$.

4.3. Joint L-System

As in the case of the double L-System, the fitting procedure of the joint L-System starts by considering the time series $\{(A_k,B_k),k=1,2,\ldots,K\}$. The L-System alphabet is inferred as the set with LG pairs (λ_l,γ_g), using the procedure of the double L-System described in Section 4.2. Thus, the arrival rates and the mean sizes are inferred independently. The identification of time scale ranges is now based on the time series of byte arrivals, i.e. $\{A_kB_k,k=1,2,\ldots,K\}$. To infer the production rules, defined by matrices $\mathbf{U}^{(r_b)}$, $r_b=1,\ldots,R_b$, data is first rounded as in the case of the double L-System. Then the probabilities are inferred as

$$u_{lmqn}^{(r_b)} = f_{lmqn}^{(r_b)} \Big/ \sum_{q=1}^{L}\sum_{n=1}^{G} f_{lmqn}^{(r_b)}, \tag{21}$$

with $l=1,\ldots,L$, $m=1,\ldots,G$ and $r_b=1,\ldots,R_b$, where $f_{lmqn}^{(r_b)}$ represents the number of times that, over all scales of range r_b, the parent $(X_{(j,r_b)}^{(i)}, Y_{(j,r_b)}^{(i)})=(\lambda_l,\gamma_m)$ produced the left child $(X_{(j-1,r_b')}^{(2i-1)}, Y_{(j-1,r_b')}^{(2i-1)})=(\lambda_q,\gamma_n)$.

4.4. L-System with PMFs

The L-System characterizing the packet arrival process is inferred exactly as in the case of the single L-System (Section 4.1). Note that this first step implicitly associates each individual packet (at the finest time scale) with an arrival rate. The inference of the packet size process starts by considering the time series of (individual) packet sizes $\{C_n,n=1,2,\ldots,N\}$, where C_n is the size of the nth packet and N is the total number of packets. We then partition this time series into L subsets defined by

$$D^l = \{C_n : L(n)=\lambda_l,\ n=1,2,\ldots,N\}, \quad l=1,2,\ldots,L, \tag{22}$$

where $L(n)$ represents the arrival rate that has been associated to the nth packet. Thus subset D^l collects the sizes of all (individual) packets that were assigned an arrival rate λ_l. These subsets will be used to infer alphabets of (individual) packet sizes for each arrival rate. Specifically, we determine from each D_l the Q_l most frequent packet size values (e.g. using histograms) and collect them in alphabet $\Upsilon^l=\{v_1v_2,\ldots,v_{Q_l}\}$. At this point, we round each element of D^l to the nearest element in Υ^l, resulting in new subsets

$$\tilde{D}^l = \{\Phi_{\Upsilon^l}(x), x\in D^l\}, \quad l=1,2,\ldots,L. \tag{23}$$

Finally, we infer for each set $\tilde{D}^l$ the corresponding PMF $h^l(e)=P\{E_1=e\}, e\in\Upsilon^l$.

5. Numerical results

We have applied our fitting procedures to four traces: (i) the well-known pOct Bellcore trace, (ii) one IP trace measured at the University of Aveiro (UA), (iii) one IP trace measured at a Portuguese ADSL ISP, representing the usage of Kazaa by a group of 10 users, and (iv) a IP trace measured in the same ISP, rep-resenting the usage of the online game operation flashing point (OFP) also by a group of 10 users. The sampling interval was 0.1 s in all traces. The UA trace is representative of Internet access traffic produced within a University campus environment. The University of Aveiro is connected to the Internet through a 10 Mb/s ATM link and the measurements were carried out in a 100 Mb/s Ethernet link connecting the border router to the firewall, which only transports Internet access traffic. The traffic analyzer was a 1.2 GHz AMD Athlon PC, with 1.5 GB of RAM, running WinDump. The measurements recorded the arrival instant and the IP header of each packet. WinDump reported no packet drops during the measurement periods. The main characteristics of the used traces are summarized in Table 1. Note that for the Bellcore trace the measured sizes correspond to Ethernet packet sizes and for the remaining traces correspond to IP packet sizes.

5.1. Single L-System

The pOct trace was fitted to an alphabet of $L=234$ arrival rates ranging from 4 and 2364 pkts/s with a step of 10 pkts/s (because it corresponds to one arrival in the sampling interval). The logscale diagram identified four time scale

Table 1
Main characteristics of measured traces

Trace name	Capture period	Trace size (pkts)	Mean rate (byte/s)	Mean packet size (bytes)
pOct	Bellcore trace	1 million	362,750	568
UA	12.41 p.m. to 14.27 p.m., July 6th 2001	7 millions	654,780	600
Kazaa	10.26 p.m. to 12.13 p.m., October 18th 2002	1 million	194,670	1225
OFP	10.26 p.m. to 12.02 p.m., October 18th 2002	0.5 million	72,552	803

ranges (within a total of 14 time scales) defined by $j_1=3$, $j_2=6$, $j_3=8$, $j_4=9$ and $j_5=14$. In the case of the UA trace the fitted alphabet had $L=215$ arrival rates, ranging from 441 to 2581 pkts/s, in steps of 10 pkts/s. As referred before, the UA trace has three time scale ranges (Fig. 5). The Kazaa and OFP traces were fitted to alphabets of $L=32$ arrival rates. These traces revealed the same two time scale ranges, defined by $j_1=5$ and $j_2=13$.

5.2. Double L-System

The L-Systems modeling the packet arrival process were those inferred for the single L-System model. The packet size process of the pOct trace was fitted to an alphabet of $G=50$ mean packet sizes, ranging from 64 to 1436 bytes in steps of 28 bytes. We identified three timescale ranges defined by $j_1=3$, $j_2=8$ and $j_3=14$. The UA trace was fitted to an alphabet of $G=50$ mean packet sizes, ranging from 232 bytes to 1016 bytes in 16 bytes steps. Again three timescale ranges were identified, defined by $j_1=3$, $j_2=8$ and $j_3=17$. For the Kazaa and OFP traces we obtained alphabets with $G=30$, ranging, respectively, from 29 bytes to 1537 bytes in steps of 52 bytes and from 23 bytes to 1531 bytes in steps of 52 bytes. In the Kazaa trace four timescale ranges were identified (defined by $j_1=3$, $j_2=8$, $j_3=9$ and $j_4=14$) but in the OFP trace only two were identified (defined by $j_1=5$ and $j_2=14$).

5.3. Joint L-System

For each trace, the alphabets of the joint L-System was inferred as all possible combinations of the alphabets, for arrivals and sizes, obtained in the previous two models. The analysis of the (second-order) logscale diagram of the byte arrival process identified the following time scale ranges: (i) for the pOct trace the four timescale ranges $j_1=5$, $j_2=8$, $j_3=9$, $j_4=14$; (ii) for the UA trace also four ranges defined by $j_1=5$, $j_2=8$, $j_3=9$, $j_4=14$; (iii) for the Kazaa trace only two ranges defined by $j_1=5$, $j=2=14$ and (iv) for the OFP trace the three ranges $j_1=5$, $j_2=11$, $j_3=14$.

5.3.1. L-System with PMFs

As in the double L-System case, the L-Systems modeling the packet arrival process were those inferred for the single L-System model. To infer the packet size PMFs, we have considered the same set of packet sizes for all arrival rates. Also, in all traces, only the 20 most frequent packet sizes were considered. The inferred packet size sets were: $\Psi^l=\{64, 74, 94, 102, 110, 126, 130, 142, 150, 162, 174, 190, 570, 938, 986, 1082, 1090, 1242, 1282, 1518\}$ for the pOct trace, $\Psi^l=\{40, 48, 52, 60, 77, 114, 213, 351, 386, 552, 576, 608, 628, 837, 932, 1216, 1400, 1420, 1462, 1500\}$ for the UA trace, $\Psi^l=\{40, 48, 52, 124, 236, 576, 776, 808, 1084, 1176, 1362, 1400, 1420, 1440, 1442, 1454, 1462, 1476, 1480, 1492\}$, for the Kazaa trace and $\Psi^l=\{40, 44, 48, 52, 208, 636, 648, 668, 674, 686, 708, 710, 1064, 1418, 1420, 1442, 1454, 1460, 1480, 1492\}$ for the OFP trace.

5.4. Model comparison

The parameter estimation took, in all cases, less than 2 min, using a MATLAB implementation running in the PC described above. This shows that the fitting procedures are computationally very efficient (note that the size of the alphabet, the number of ranges and the size of the trace, which determine the computational time, are all relatively large).

The suitability of the traffic models and the accuracy of the fitting procedures was assessed using several criteria. For the original data traces and for traces synthesized according to the inferred models, we compare both the PMF of the byte arrival process and the autocovariance functions of the byte arrival, packet arrival and packet size processes. For the same two traces, we compare the queuing behavior, assessed by the packet loss ratio and by the average packet delay estimated through trace-driven simulation. In the case of the single L-System, we have considered a fixed packet length equal to the mean packet size of the original data. For the pOct Bellcore trace, we also considered a special case of the L-System with PMFs model with only one PMF (for packet sizes), i.e. with no dependence between arrivals and sizes. Note that this special model is only able to characterize the packet size distribution; it will not capture the autocovariance and the multifractal behavior of the packet size process, nor the correlations between arrivals and sizes.

Fig. 6 shows that, in the case of the pOct trace, all models were able to match relatively well the PMF of the byte arrival process. The agreement is not so good in the case of the autocovariance functions. In the packet arrival process (Fig. 7), there is a relatively good match for all models because all of them include an L-System of arrival rates. In the packet size process (Fig. 8), there is a good agreement

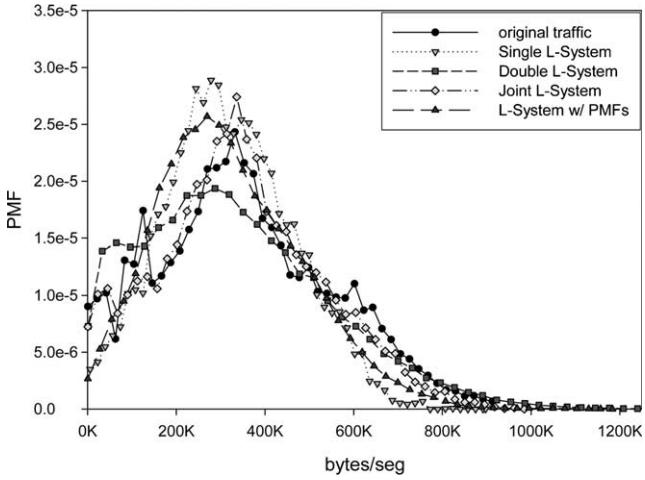

Fig. 6. Probability mass function, trace pOct.

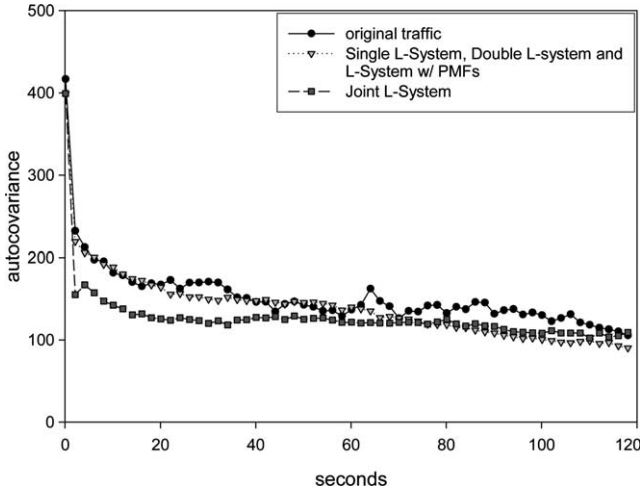

Fig. 7. Packet arrival process autocovariance functions, trace pOct.

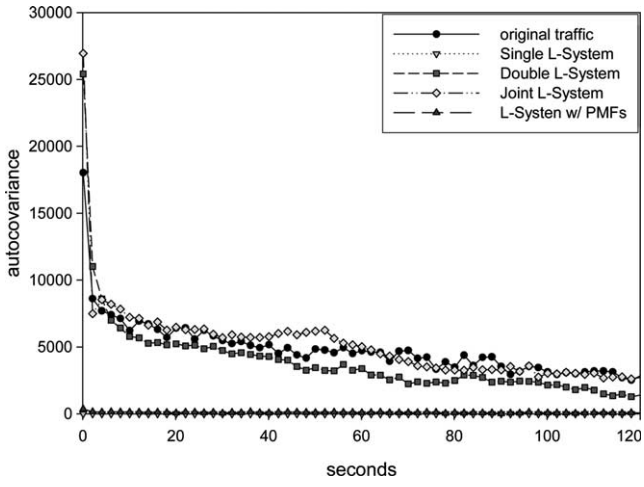

Fig. 8. Packet size autocovariance functions, trace pOct.

except in the case of the L-System with PMFs. This model has null autocovariance for all positive lags, which is not the case of both the double and joint L-System models where the autocovariance of the packet size process is implicitly

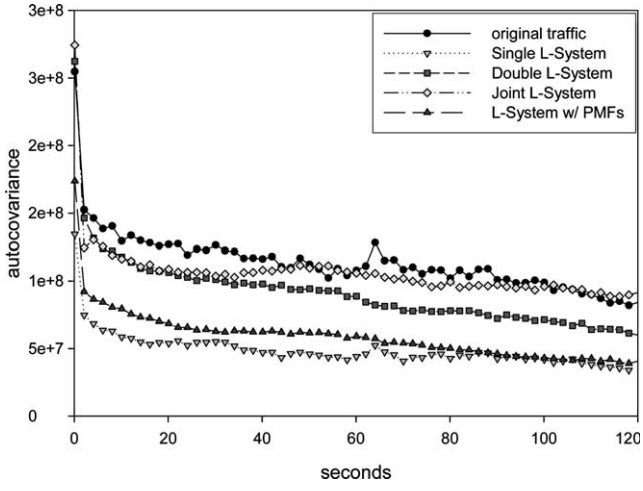

Fig. 9. Byte arrival process autocovariance function, trace pOct.

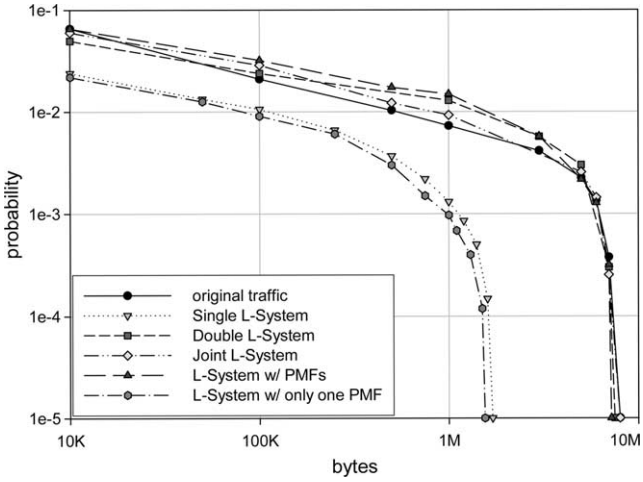

Fig. 10. Packet loss ratio versus buffer size, trace pOct.

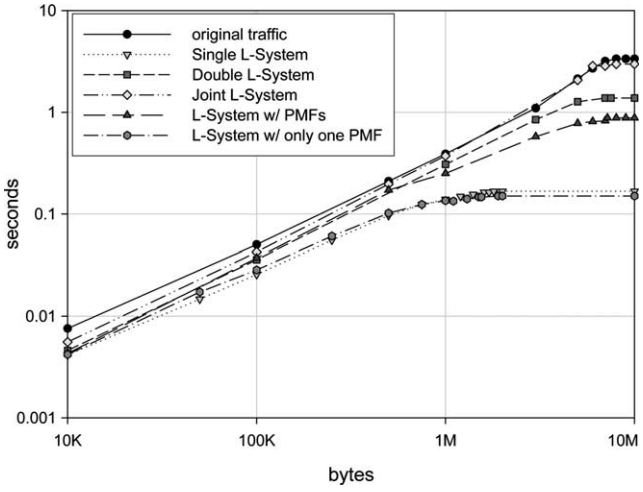

Fig. 11. Average packet delay versus buffer size, trace pOct.

driven by the cascaded structure of the L-System for mean packet sizes. In the byte arrival process (Fig. 9), a good agreement was only obtained in the case of the joint L-System model. This model is the most complete one since

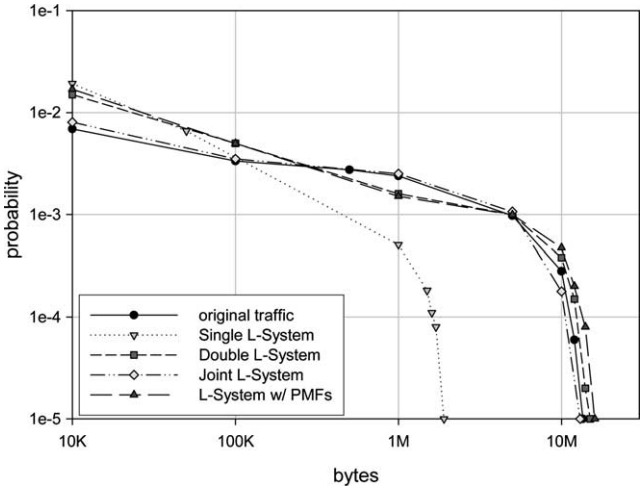

Fig. 12. Packet loss ratio versus buffer size, trace UA.

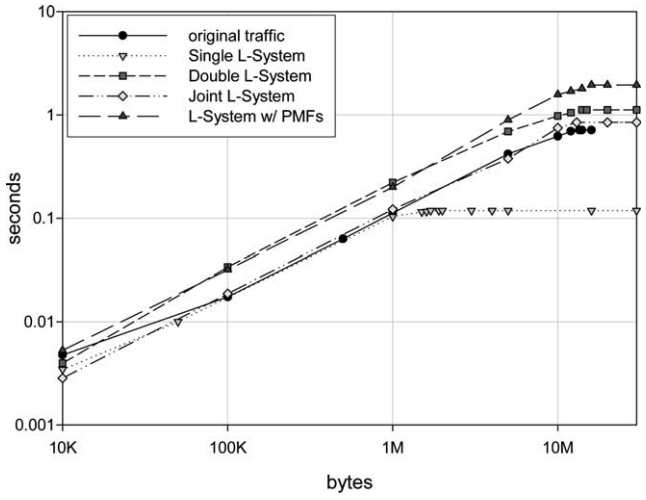

Fig. 13. Average packet delay versus buffer size, trace UA.

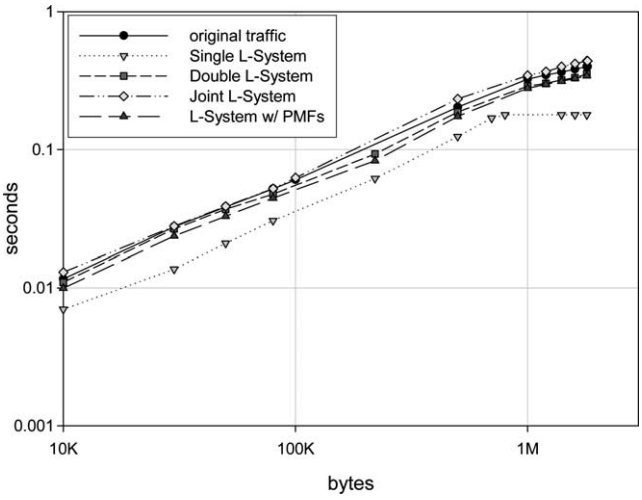

Fig. 15. Average packet delay versus buffer size, trace Kazaa.

it is able to capture the autocovariance of the packet arrival and packet size processes, correlations between arrivals and sizes and multifractal behavior on the byte arrival process. Note that in the case of the double L-System, although there is a good agreement both in the packet arrival and packet size processes, there is a deviation in the case of the byte arrival process. This clearly illustrates the importance of modeling the correlations between arrivals and sizes, since the lack of such ability is the only difference between the double and the joint L-System models. Similar results were obtained for the other traces.

The multifractal characteristics of the packet arrival process were assessed using a linear multiscale diagram [7], which plots $h_q = \alpha_q/q$ against q; α_q represents the qth order scaling exponent, estimated in the qth order logscale diagram. Multifractal scaling behavior is detected when there is no *horizontal* alignment (within the limits of the 95% confidence intervals). Fig. 18 shows that the packet arrival processes of the UA and Kazaa traces, and of the traces synthesized according to the inferred L-System, all

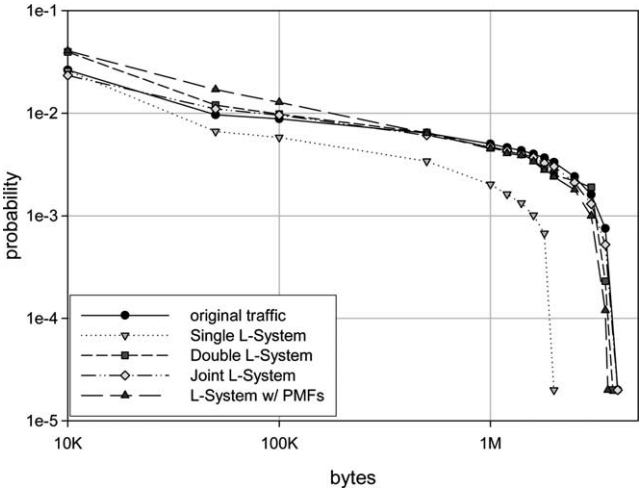

Fig. 16. Packet loss ratio versus buffer size, trace OFP.

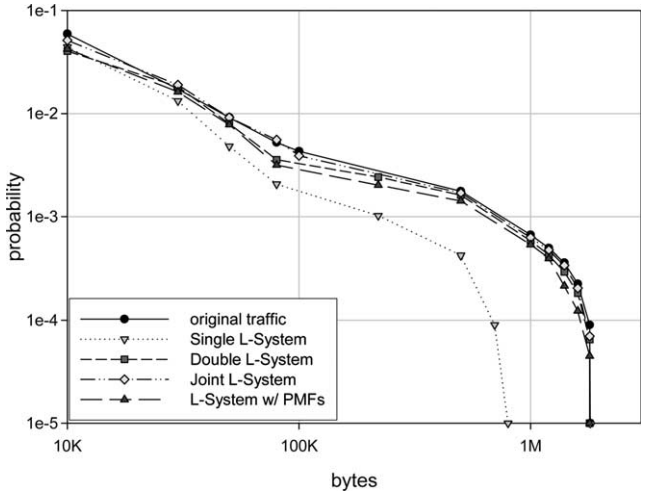

Fig. 14. Packet loss ratio versus buffer size, trace Kazaa.

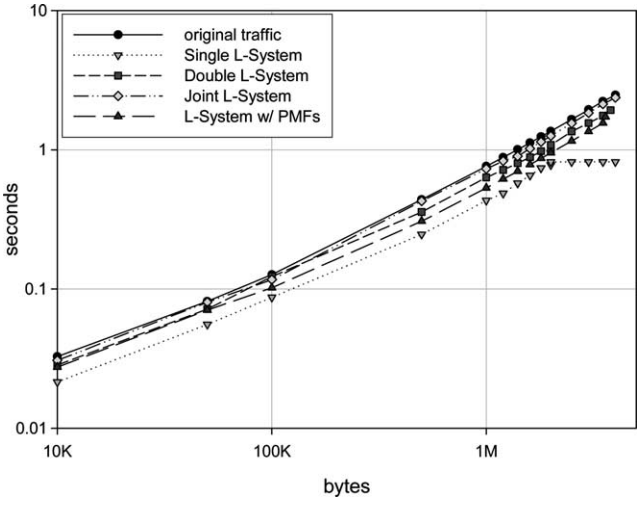

Fig. 17. Average packet delay versus buffer size, trace OFP.

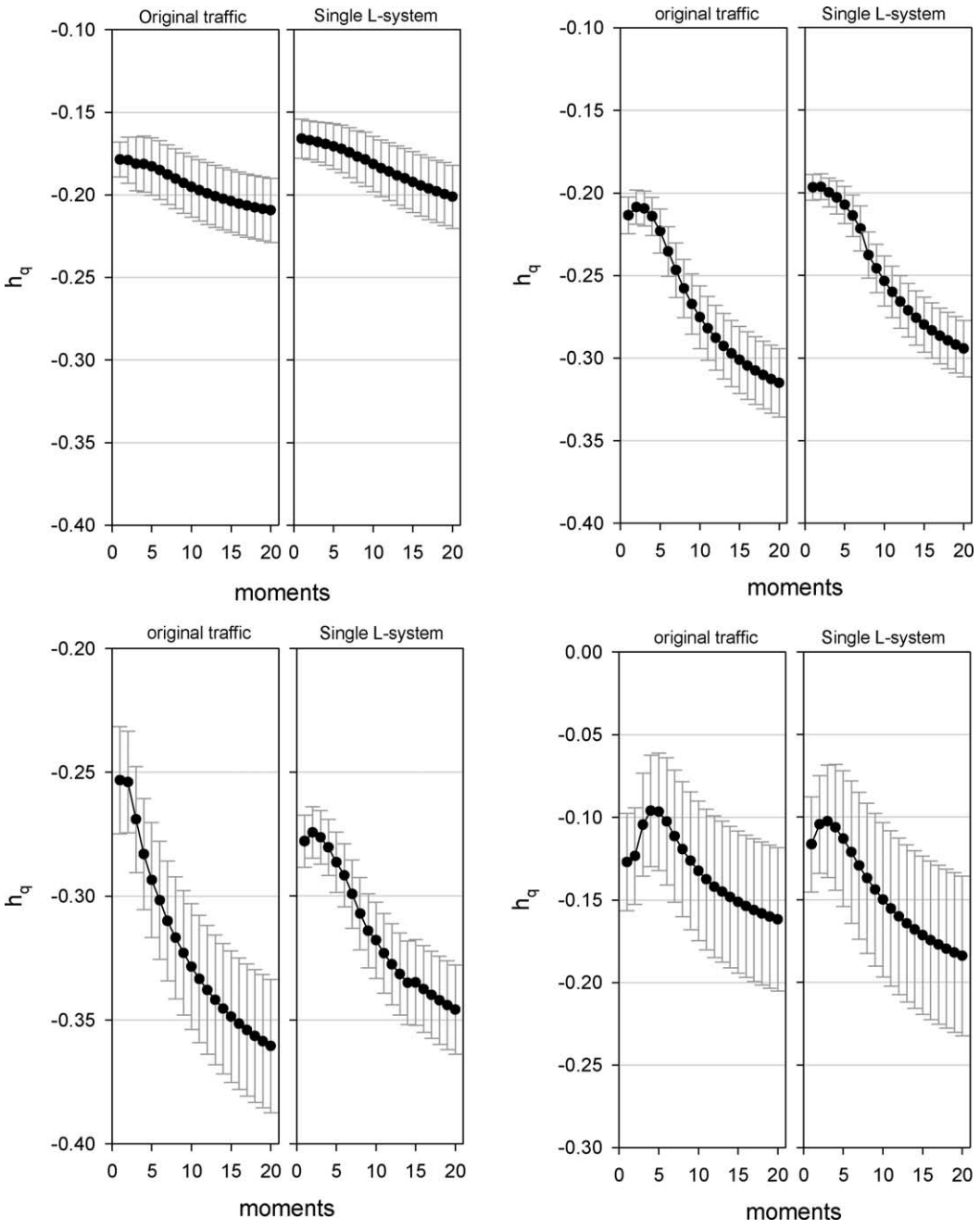

Fig. 18. Linear multiscale diagrams of the packet arrival process, with 95% confidence intervals (from left to right and from top to bottom) trace pOct, trace UA, trace Kazaa and trace OFP.

have multifractal scaling behavior. The pOct trace is not multifractal and the OFP trace is in the limit between non-trivial and trivial multifractality. For all traces, and independently of the presence of multifractal scaling behavior, the L-System was able to capture the scaling behavior of the original traces, since the curves of the original traces are very similar to the ones of the fitted traces.

To assess queuing behavior the buffer size was varied from 10KB to 20 MB. The service rate was 518KB/s for the pOct trace (corresponding to all utilization of 0.7) and 726KB/s for the UA trace (corresponding to an utilization of 0.9). Figs. 10–13 show that, for all traces, the fitting of the queuing behavior was very good for the joint L-System model but slight differences occurred for the double L-System and the L-System with PMFs. The single L-System and L-System with only one PMF both achieve a similar performance with a large deviation from the original data. This clearly shows the importance of characterizing the correlations between arrivals and sizes. We have also analyzed the queuing behavior of the Kazaa and OFP traces (for utilizations of 0.7). The results are

shown in Figs. 14–17. In these cases, there is a good matching for all L-System models (characterizing both the packet arrivals and packet sizes) but again the best match is obtained with the joint L-System model.

From these results, we conclude first that it is important to characterize both the packet arrival and packet size processes and their correlations. The best model, which was able to track almost perfectly the queuing behavior of all traces, is the joint L-System. This can be attributed to its ability of capturing correlations between arrivals and sizes, as well as multifractal behavior on the byte arrival process. The double L-System is somewhat impaired by its inability to capture these correlations and the L-System with PMFs by its inability to capture the autocovariance and the multifractal behavior of the packet size process. However, the L-System with PMFs has a lower number of parameters and therefore can be considered a good alternative. When the alphabet of arrivals has L elements, the alphabet of sizes has G elements and there are R time scale ranges, the number of parameters of the L-System with PMFs is L^2R+GL and the one of the joint L-System is G^2L^2R.

6. Conclusions

In this paper, we compared four traffic models, and associated parameter fitting procedures, based on so-called Lindenmayer Systems (L-Systems), which were introduced by biologist A. Lindenmayer as a method to model plant growth. One traffic model characterizes the packet arrival process and the remaining three characterize both the packet arrival and the packet size processes. These models are able to capture the multiscaling and multifractal behavior sometimes observed in Internet traffic. We applied the models to measured traffic data: the well-known pOct Bellcore, a trace of aggregate WAN traffic and two traces of specific applications (Kazaa and OFP). We assessed the multifractality of these traces using Linear Multiscale Diagrams. The suitability of the traffic models was evaluated by comparing the empirical and fitted probability and autocovariance functions; we also compared the packet loss ratio and average packet delay obtained with the measured traces and with traces generated from the fitted models. Our results highlight the importance of characterizing both the packet arrival and packet size processes and show that L-System based traffic models that have these characteristics can achieve very good fitting performance in terms of first- and second-order statistics and queuing behavior.

References

[1] P. Salvador, A. Pacheco, R. Valadas, Modeling IP traffic: joint characterization of packet arrivals and packet sizes using BMAPs, Computer Networks Journal 44 (3) (2004) 335–352.

[2] B. Mandelbrot, Intermittant turbulence in self-similar cascades: divergence of high moments and dimensions of the carrier, Journal of Fluid Mechanics 62 (1974) 331–358.

[3] R. Riedi, J.L. Véhel, Multifractal properties of TCP traffic: a numerical study, Technical Report No. 3129, INRIA Rocquencourt, France Available at www.dsp.rice.edu/~riedi.

[4] A. Feldmann, A. Gilbert, W. Willinger, Data networks as cascades: investigating the multifractal nature of internet WAN traffic, in: Proceedings of ACM/SIGCOMM'98, Vancouver, Canada, 1998, pp. 42–55.

[5] R. Riedi, M. Crouse, V. Ribeiro, R. Baraniuk, A multifractal wavelet model with application to network traffic, IEEE Transactions on Information Theory 45 (4) (1999) 992–1018.

[6] A. Feldmann, A. Gilbert, P. Huang, W. Willinger, Dynamics of IP traffic: a study of the role of variability and the impact of control, in: ACM/SIGCOMM'99, Cambridge, MA, USA, 1999, pp. 301–313.

[7] P. Abry, P. Flandrin, M. Taqqu, D. Witch, Self Similar Network Traffic Analysis and Performance Evaluation, Wiley, New York, 2000 Wavelets for the analysis, estimation and synthesis of scaling data, pp. 39–88.

[8] J. Gao, I. Rubin, Multifractal analysis and modeling of long-range-dependent traffic, in: Proceedings ICC'99, Vancouver, Canada, 1999, pp. 382–386.

[9] A. Gilbert, W. Willinger, A. Feldmann, Scaling analysis of conservative cascades, with applications to network traffic, IEEE Transactions on Information Theory 45 (3) (1999) 971–992.

[10] A. Erramilli, O. Narayan, A. Neidhardt, I. Saniee, Performance impacts of multi-scaling in wide area TCP/IP traffic, in: Proceedings of INFOCOM'2000, Tel Aviv, Israel, 2000, pp. 352–359.

[11] D. Veitch, P. Abry, P. Flandrin, P. Chainais, Infinitely divisible cascade analysis of network traffic data, in: Proceedings of the International Conference on Acoustic Speech and Signal Processing, Istanbul, Turkey, 2000.

[12] J. Gao, I. Rubin, Multifractal modeling of counting processes of long-range-dependent network traffic, Computer Communications 24 (2001) 1400–1410.

[13] A. Lindenmayer, Mathematical models for cellular interactions in development. II. Simple and branching filaments with two-sided inputs, Journal of Theoretical Biology 18 (1968) 300–315.

[14] H. Peitgen, H. Jurgens, D. Saupe, Chaos and Fractals: New Frontiers of Science, Springer, Berlin, 1992.

[15] P. Salvador, A. Nogueira, R. Valadas, Modeling multifractal traffic with stochastic L-Systems, in: Proceedings of GLOBECOM'2002, Taipei, Taiwan, 2002.

[16] P. Salvador, A. Nogueira, R. Valadas, Modeling multifractal IP traffic: characterization of packet arrival and sizes with stochastic L-Systems, in: Proceedings of the 10th International Conference on Telecommunication Systems, Modeling and Analysis (ICTSM10), vol. 2, Monterey, CA, USA, 2002, pp. 577–587.

[17] P. Salvador, A. Nogueira, R. Valadas, Joint characterization of the packet arrival and packet size processes of multifractal traffic based on stochastic L-Systems, in: Proceedings of the 18th International Teletraffic Congress (ITC18), Berlin, Germany, 2003, pp. 561–570.

[18] P. Salvador, A. Nogueira, R. Valadas, Framework based on stochastic L-Systems for modeling IP traffic with multifractal behavior, in: Proceedings of SPIE Conference on Performance and Control of Next Generation Communication Networks, vol. 5244, ITCom 2003, Orlando, FL, USA, 2003, pp. 18–28.

[19] P. Salvador, A. Nogueira, R. Valadas, Scaling behavior analysis of multifractal traffic models based on stochastic L-Systems, Technical Report, University of Aveiro, 2002.